AIAA JOURNAL
Vol. 38, No. 3, March 2000

Dynamic Response of Adaptive Cross-Ply Cantilevers Featuring Interlaminar Bonding Imperfections

U. Icardi* and M. Di Sciuva†
Politecnico di Torino, 10129 Turin, Italy
and
L. Librescu‡
Virginia Polytechnic Institute and State University, Blacksburg, Virginia 24061-0219

The implications of slip-type interfacial bonding imperfections on the dynamic behavior of adaptive laminated beams with surface-bonded piezoactuator layers are investigated. Numerical results are supplied, and pertinent conclusions on the free and forced flexural motions under transient distributed loadings, as a function of the measure of bonding imperfections, are outlined. Near the end of this problem approach, a recently developed theory of anisotropic laminated plates that incorporates the effect of imperfect interlaminae bondings and fulfils the shear traction continuity requirements is used. The control is achieved via the action of a piezoelectrically induced bending moment at the tip of the beam, and in this context four different feedback control laws are employed. The obtained results reveal the powerful role played by the proposed control methodology toward suppressing vibrations and attenuating the detrimental effect induced by the interlaminae bonding flaws.

Introduction

THE increasingly stringent performance requirements featured by the next generation of flight and reusable launch vehicles and the hostile environments in which these are likely to operate impose considerable challenges to structural engineers and research workers involved in their design. Of great promise toward the successful solution of a number of these technical challenges is the ongoing integration in their construction of advanced laminated composites material systems. However, as was revealed quite recently,[1–6] the response behavior and the load-carrying capacity of composite material structures can be adversely affected by a variety of effects occurring at a local level, such as imperfect bonding at the interface between the constituent layers, transverse cracking, delamination, fiber breakage, etc. In such cases, to obtain a reliable prediction of the response of laminated composite structures, the perfect bonding assumptions used traditionally in the modeling of laminated composite structures, implying continuous displacements across the interfaces, no longer can be adopted. Moreover, to circumvent the deleterious effects induced by the loss of integrity of such structures and also to have the ability to adapt to changing environments, advanced control techniques have to be devised and implemented. In this sense, the structures of the new generation of flight vehicles have to incorporate integrated and highly distributed networks of sensors and actuators linked through a centralized multiprocessor.

Comprehensive reviews and assessments of the achievements reached by the use of such smart structures in aerospace applications and in flexible structures can be found, for example, in work by Crawley,[7] Rao and Sunar,[8] and Tzou.[9]

The direct and converse piezoelectric effects are basic toward the use of piezoelectric materials as sensors and actuators, respectively. Employment of a control law relating the applied electric field with one of the kinematic response quantities, according to a prescribed functional relationship,[10–14] results in dynamic eigenvalue/boundary-value problems whose solution yields the closed-loop dynamic response characteristics of the controlled structure.

Because interlayer slip causes stiffness degradation with detrimental repercussions on the overall behavior of the composite material structures encompassing their static,[1,2] dynamic, and stability responses,[4,6] the study of its implications on the dynamic response to time-dependent excitations and vibrations control of such structures would be of a significant theoretical and practical importance. In spite of this, with the exception of Ref. 15, to the best of authors' knowledge, studies of the control of the dynamic response of damaged beams to transient loadings are absent in the specialized literature. The aim of the present paper is to fill the existing gap by supplying pertinent information on this topic.

A study of the enhancement of the dynamic response of cantilevers to transient loadings via the implementation of the adaptive capability, referred to as induced strain actuation, is addressed. As is well known, cantilevers are used often in engineering, serving as a basic model for a number of constructions used in the aeronautical and space industries, such as airplane wings, helicopter blades, robotic manipulator arms and space booms, as well as in many mechanical engineering applications.

The theory of damaged multilayered beams used is based on that developed by Di Sciuva et al.[4] and by Di Sciuva,[5] which represents the further development of earlier ones due to Cheng et al.[1,2] and Schmidt and Librescu.[3]

As a preparatory step, the basic kinematic relations of laminated damaged beams and a rather short derivation of the pertinent governing equations will be presented (for details, see Refs. 4 and 5). In the forthcoming development three related issues will be addressed, namely, 1) the development of an efficient mathematical methodology for determining the closed-loop dynamic response of multilayered orthotropic cantilever beams to time-dependent external excitations, 2) the assessment of the efficiency of the proposed control methodology, and 3) the influence of interface bonding defects on the closed-loop dynamic response characteristics of the strutures.

Structural Model

A multilayered composite cross-ply beam of length L and of solid rectangular cross section (of dimensions $b \times h$), consisting of a finite number $\mathcal{N}$ of linearly elastic orthotropic layers of uniform thickness $^{(k)}h\ (k = \overline{1, \mathcal{N}})$ is considered. One assumes that piezoactuator layers are bonded on the upper and lower faces of the beam and are spread over its entire span.

Received 7 December 1998; revision received 20 July 1999; accepted for publication 2 August 1999.

*Assistant Professor, Department of Aerospace Engineering, Corso Duca degli Abruzzi 24.
†Associate Professor, Department of Aerospace Engineering, Corso Duca degli Abruzzi 24.
‡Professor, Department of Engineering Science and Mechanics.

Preliminaries and Notations

The points of the beam are referred to an orthogonal Cartesian coordinate system (x, y, z), with (x, y) the reference plane, assumed to be the midplane, with y and z the cross-sectional coordinates, and with x the spanwise coordinate. The distances along z between the reference plane and the undeformed top and bottom faces of the kth layer are ${}^{(k)}Z^{+}$ and ${}^{(k)}Z^{-}$, respectively.

It is assumed that the material of each layer of the host structure features orthotropic properties and that the anisotropy of the piezoactuators is of the transversal isotropic type, with the surface of isotropy parallel to (x, y). It is also assumed that the z axis coincides with the direction of polarization and that $\mathcal{E}_z$ is the only component of the electric field vector. Under these assumptions, the following stress–strain relations hold valid for the piezoelectric layers:

$$\sigma_{xx} = \tilde{\sigma}_{xx} + \hat{\sigma}_{xx} = \bar{Q}_{11}\epsilon_{xx} - \bar{e}_{zx}\mathcal{E}_z, \qquad \sigma_{xz} = \tilde{\sigma}_{xz} = 2\bar{Q}_{44}\epsilon_{xz} \tag{1}$$

where $\tilde{\sigma}_{xx}$ and $\hat{\sigma}_{xx}$ are the mechanical and piezoelectric contributions to the total stress, respectively. $\bar{Q}_{11}$ and $\bar{Q}_{44}$ are the reduced components of the stiffness tensor, and $\bar{e}_{zx}$ is the reduced piezoelectric constant.[9]

In light of Eq. (1), $\hat{\sigma}_{xx}$ is the only piezoelectrically induced stress and is proportional to the applied electric field $\mathcal{E}_z$, assumed constant through the thickness of piezoactuators. Equation (1) also applies to the layers of the host structure, provided that the contribution $\hat{\sigma}_{xx}$ is discarded.

Kinematics

The beam structural model used is of the third order and incorporates the following features: 1) orthotropy of constituent material layers, 2) transverse shear deformability, 3) distortion of the deformed normals, and 4) interface bonding damage of the sliding type. The latter feature involves the existence of an interlaminar jump of the spanwise displacement $U(x, z, t)$ across the laminae interfaces[1–6]:

$${}^{(k)}\mathcal{V} = U|_{(z={}^{(k+1)}Z^{-})} - U|_{(z={}^{(k)}Z^{+})}$$

where ${}^{(k)}\mathcal{V}$ is the jump in the displacements at the interface between the kth and $(k+1)$th layers. Furthermore, the shear traction continuity requirement at the interfaces

$$\sigma_{xz}|_{(z={}^{(k)}Z^{+})} = \sigma_{xz}|_{(z={}^{(k+1)}Z^{-})}$$

and the free-shear condition at the upper, that is, $z = h/2$, and lower, that is, $z = -h/2$, surfaces of the beam

$$\sigma_{xz}(x, -h/2, t) = \sigma_{xz}(x, h/2, t) = 0$$

should be fulfilled.

In view of the preceding statements and to reduce the three-dimensional elastic problem to an equivalent one-dimensional one, the following representation for the spanwise U and transverse W displacements is postulated:

$$U(x, z, t) = u(x, z, t) + \mathcal{U}(x, z, t) + \mathcal{V}(x, z, t) \tag{2}$$

$$W(x, z, t) = w(x, t) \tag{3}$$

The three terms intervening in Eq. (2) are detailed as follows.

The first term, namely,

$$u(x, z, t) = u^{(0)} + z(\phi_x - w_{,x}) + z^2(F + z\mathcal{F})\phi_x \tag{4}$$

is consistent with the classical expansion used in the third-order single layer or smeared laminate models. It gives a contribution to the spanwise displacement that is continuous and has a continuous first derivative in the thickness coordinate z. The generalized displacements are defined as follows: $u^{(0)} = u^{(0)}(x, t)$ is the spanwise displacement at the midplane, $\phi_x = \phi_x(x, t)$ is the transverse shear rotation of the normal at the midplane, and $w = w(x, t)$ is the transverse deflection at the midplane. F and $\mathcal{F}$ are constants whose values are determined as to fulfill the free-shear condition on the upper and lower free surfaces:

$$F = -\frac{1}{2h}\sum_{k=1}^{\mathcal{N}-1} {}^{(k)}a, \qquad \mathcal{F} = -\frac{4}{3h^2}(1 - hF) \tag{5}$$

Here, ${}^{(k)}\hat{a}$ are constants, called the continuity constants, that depend only on the transverse shear mechanical properties of the constituent layers, namely, ${}^{(k)}\bar{Q}_{44}$, and that are determined as the shear traction continuity requirement is met at the interfaces. Details on their derivation are given in Ref. 16. Note that, for symmetric layups,

$$\sum_{k=1}^{\mathcal{N}-1} {}^{(k)}a = 0$$

which implies $F = 0$ and $\mathcal{F} = -(4/3h^2)$.

The second term[17–21]

$$\mathcal{U}(x, z, t) = \phi_x \sum_{k=1}^{\mathcal{N}-1} {}^{(k)}a\left(z - {}^{(k)}Z^{+}\right)\mathcal{H}_k \tag{6}$$

gives a contribution that is continuous, but with discontinuous first derivative with respect to the z coordinate, enabling one to meet the shear traction continuity requirement with suitably defining the continuity constants ${}^{(k)}a$ (Ref. 16) and featuring the distorsion of the normal. Herein, $\mathcal{H}_k$ is the Heaviside unit step function.

The third term

$$\mathcal{V}(x, z, t) = \sum_{k=1}^{\mathcal{N}-1} {}^{(k)}\mathcal{V}(x, t)\mathcal{H}_k \tag{7}$$

represents the jump of the spanwise displacement component across the interfaces, enabling one to incorporate the bonding imperfection effect of the slip type in the model.

In accordance to the previous studies in the field (e.g., Refs. 1–6), we postulate for the interlaminar displacement jump ${}^{(k)}\mathcal{V}$ at the interface between contiguous layers k and $k+1$, a linear shear slip law:

$${}^{(k)}\mathcal{V}(x, t) = {}^{(k)}\mathcal{R}\sigma_{xz}\left(x, {}^{(k)}Z, t\right) \tag{8}$$

where ${}^{(k)}\mathcal{R} \geq 0$ is the sliding constant between the kth and $(k+1)$th layers.

Note that in addition to the two extreme situations corresponding to 1) the perfect bonding assumption, that is, ${}^{(k)}\mathcal{R} = 0$, yielding ${}^{(k)}\mathcal{V} = 0$, and 2) the completely debonding interfaces, that is, delamination ${}^{(k)}\mathcal{R} = \infty$, yielding $\sigma_{xz}(x, {}^{(k)}Z, t) = 0$, Eq. (8) also covers the intermediate cases of imperfectly bonded interfaces (${}^{(k)}\mathcal{R} \neq 0, \infty$). With a suitable choice of ${}^{(k)}\mathcal{R}$, the effects of an internal defect, such as transverse cracking, delamination, and fiber breakage, can be accounted for. This constitutes an alternative to the compliant layer approach,[22] where a fictitious compliant layer with material properties suitably selected so as to simulate the stiffness degradation induced by such defects is embedded in the composite.

A great deal of experimental work directed toward characterization of the damage via nondestructive techniques has been accomplished. In this sense, some of the proposed techniques could be able to correlate the degree of sliding with the parameter ${}^{(k)}\mathcal{R}$. The reader is referred to Lavrentyev and Rokhlin,[23] where a presentation of the state of the art on this matter and references to the pertinent literature are supplied.

By the taking into account of the various contributions, the spanwise displacement can be rewritten in compact form as follows:

$$U(x, z, t) = u^{(0)} - zw_{,x} + \mathcal{L}(z)\phi_x \tag{9}$$

where for the function $\mathcal{L}(z)$ the following expression holds:

$$\mathcal{L}(z) = z + Fz^2 + \mathcal{F}z^3 + \sum_{k=1}^{\mathcal{N}-1} {}^{(k)}\hat{a}\left(z - {}^{(k)}Z^{+}\right)\mathcal{H}_k + \bar{\mathcal{V}} \tag{10}$$

where $\bar{\mathcal{V}}(z)$ is

$$\bar{\mathcal{V}}(z) = \sum_{k=1}^{\mathcal{N}-1} {}^{(k)}\bar{\mathcal{V}}(z)\mathcal{H}_k = \sum_{k=1}^{\mathcal{N}-1} {}^{(k)}\mathcal{R}^{(k)} Q_{44} \times \left[1 + 2^{(k)}ZhF + 3^{(k)}Z^2\mathcal{F} + \sum_{k=1}^{\mathcal{N}-1} {}^{(k)}\hat{a}\mathcal{H}_k\right]\mathcal{H}_k \tag{11}$$

Note from the preceding equation that the only component of the generalized displacement appearing in the displacement jump $\bar{\mathcal{V}}$ is the transverse shear rotation ϕ_x. Also note that, as evidenced by Eqs. (10) and (11), all of the quantities accounting for the effect of bonding imperfections that will be defined in the remainder of the paper will be those associated with the function $\mathcal{L}$, wherein the contribution $\bar{\mathcal{V}}$ of the interlaminar displacement jump is enclosed.

Governing Equations

By using the dynamic version of the principle of virtual displacements,[5] the equations of motion and the variationally consistent boundary conditions are obtained in terms of mechanical,

$$(\tilde{N}; \tilde{M}; \tilde{S}; \tilde{T}) = \langle \tilde{\sigma}_{xx}(1; z; \mathcal{L}); \sigma_{xz}\mathcal{L}_{,z}\rangle \tag{12}$$

and piezoelectrically induced,

$$(\hat{N}; \hat{M}) = \langle \bar{e}_{zx}\mathcal{E}_z(1; z)\rangle \tag{13}$$

stress resultants and stress couples. Here the operator $\langle \cdots \rangle$ indicates the stepsize integration through the beam thickness

$$\langle \cdots \rangle = b\sum_{k=1}^{\mathcal{N}} \int_{{}^{(k)}z^-}^{{}^{(k)}z^+} (\cdots)\,\mathrm{d}z$$

To express the governing equations in terms of displacement quantities, the equations of motion and the boundary conditions have to be supplemented by the constitutive equations. When this has been accomplished, the governing equations in terms of displacement quantities read

$$Au^{(0)}_{,xx} + D\phi_{x,xx} - Bw_{,xxx} = m_0\ddot{u}^{(0)} + \mu_0\ddot{\phi}_x - m_1\ddot{w}_{,x} + \hat{N}_{,x} \tag{14}$$

$$Bu^{(0)}_{,xxx} + E\phi_{x,xxx} - Cw_{,xxxx} = -\bar{P}_z + m_1\ddot{u}^{(0)}_{,x} + \mu_1\ddot{\phi}_{x,x} - m_2\ddot{w}_{,xx} + m_0\ddot{w} + \hat{M}_{,xx} \tag{15}$$

$$Du^{(0)}_{,xx} + F\phi_{x,xx} - Ew_{,xxx} - H\phi_x = \mu_0\ddot{u}^{(0)} + \pi_0\ddot{\phi}_x - \mu_1\ddot{w}_{,x} \tag{16}$$

In these equations, the one-dimensional stiffness quantities are defined as follows:

$$(A; B; C; D; E; F) = \langle \bar{Q}_{11}(1; z; z^2; \mathcal{L}; z\mathcal{L}; \mathcal{L}^2)\rangle$$
$$H = \langle \bar{Q}_{44}\mathcal{L}^2_{,z}\rangle \tag{17}$$

and the inertia terms

$$(m_i; \mu_i; \pi_i) = \langle {}^{(k)}\rho z^i(1; \mathcal{L}; \mathcal{L}^2)\rangle \tag{18}$$

where ${}^{(k)}\rho$ is the mass density of the kth layer. $\bar{P}_z$ is the transversal distributed time-dependent load acting on the beam. Note that the effects of sliding imperfections are included in the last four stiffness quantities of Eqs. (12) and (13) and in the last two mass terms appearing in Eq. (18), where the quantity $\mathcal{L}$ [see Eq. (10)] is involved.

As also emphasized in Refs. 1–6, as a result of the inclusion of sliding imperfections, no increase in the order of the governing system occurs. Also note that under a uniform spanwise activation $\mathcal{E}_z(x, z, t) = \mathcal{E}_z(t)$, the piezoelectrically induced force $\hat{N}$ and couple $\hat{M}$, being constant with respect to x, become immaterial in the equations of motion.

Under out-of-phase activation,[10] the only piezoelectrically induced quantity that survives is the bending moment at the beam tip, $\hat{M}$, which is referred to as the boundary moment control. The case of the out-of-phase activation will be adopted here. For this specific case, the boundary conditions for the cantilever beam are

$$x = 0: \quad u^{(0)} = \phi_x = w = w_{,x} = 0 \tag{19}$$

$$x = L: \quad \tilde{N} = \tilde{S} = \tilde{T} = 0, \qquad \tilde{M} = \hat{M} \tag{20}$$

with the piezoelectrically induced bending moment $\hat{M}$ appearing as a nonhomogeneous term at $x = L$.

Control Law

To enhance the free vibration behavior, inhibit the forced vibration response to external time-dependent excitation, and prevent resonance, a suitable feedback control law relating the applied electric field $\mathcal{E}_z$ to the mechanical quantities characterizing the beam's response has to be implemented.

The control via a boundary moment acting at the beam tip is a methodology substantiated mathematically by Lagnese and Lions[24] and Lagnese[25] and proved to be efficient for the control of the dynamic response of cantilevered beams to transient loads.[10–14] To increase the control authority, a combined feedback control

$$\hat{M}(L, t) = \mathcal{K}_w w(L, t) + \mathcal{K}_v\dot{w}(L, t) + \mathcal{K}_a\ddot{w}(L, t) + \mathcal{K}_m\mathcal{M}(0, t) \tag{21}$$

is used where $\mathcal{K}_w$, $\mathcal{K}_v$, $\mathcal{K}_a$, and $\mathcal{K}_m$ are the displacement, velocity, acceleration, and moment feedback gains, respectively. Special cases of this control law have been used by Librescu et al.,[13,14] Bailey and Hubbard,[26] Tzou and Zhong,[27] and Baz.[28]

Based on Eq. (21), single and combined control laws can be implemented. Hereafter, the cases involving a single feedback control gain appearing in the same succession as in Eq. (21) will be referred to as displacement, velocity, acceleration, and moment control, respectively.

Solution Methodology

The closed-loop boundary-value/eigenvalue problems consist of the equations of motion [Eqs. (14–16)], of the boundary conditions [Eqs. (19) and (20)], and the feedback control law [Eq. (21)]. Their solution constitutes a rather intricate mathematical problem. Needless to say, derivation of exact solutions is precluded. An approximate solution is obtained via Galerkin's technique. To this end, the following steps are implemented. The first step consists of the discretization of the problem. This is accomplished by expressing the generalized displacements $u^{(0)}$, ϕ_x, and w in terms of a combination of spatial trial functions $\mathcal{G}_j(x)$ and $\mathcal{W}_j(x)$, with unknown modal amplitudes as coefficients, and of generalized coordinates $q_j(t)$. The generalized displacements have to be chosen to fulfill all of the kinematic boundary conditions of Eqs. (19) and (20), whereas the determination of the modal amplitudes constitutes the central goal of the dynamic response problem. Consequently, we have

$$\left[u^{(0)}(x, t); \phi_x(x, t); w(x, t)\right] = \sum_{j=1}^{\mathcal{J}} [\mathcal{G}_j(x); \mathcal{G}_j(x); \mathcal{W}_j(x)]\, q_j(t) \tag{22}$$

To satisfy exactly the kinematic boundary conditions at the beam root $x = 0$, $\mathcal{W}_j$ are selected as the Williams polynomials

$$\mathcal{W}_j(x) = 1 - (j + 3)x/L - (1 - x/L)^{(j+3)}$$

whereas $\mathcal{G}_j = \mathcal{W}_{j,x}$ are the x derivatives of $\mathcal{W}_j$.

As the second step, the representation given by Eq. (22) together with that resulting for the boundary moment $\hat{M}$ [Eq. (21)], and the specific expression of the time-dependent external loading $\bar{P}_z$ are replaced in the equations of motion [Eqs. (14–16)].

In general, the displacement representation of Eq. (22) does not fulfill the boundary conditions (20) at the beam tip $x = L$. However, in view of the application of Galerkin's generalized method,[29] corrective terms appear automatically in $\boldsymbol{K}$ that compensate for the nonfulfillment of these boundary conditions.

As a result, the following final matrix form of the governing equations is obtained:

$$\boldsymbol{M}\ddot{\boldsymbol{q}} + \boldsymbol{C}\dot{\boldsymbol{q}} + \boldsymbol{K}\boldsymbol{q} - \boldsymbol{F} = \boldsymbol{0} \tag{23}$$

which constitutes a set of coupled ordinary differential equations. Here $\boldsymbol{q}$ is a $3\mathcal{J} \times 1$ column matrix whose elements are $q_j(t)$; $\boldsymbol{M}$, $\boldsymbol{C}$, and $\boldsymbol{K}$ are $3\mathcal{J} \times 3\mathcal{J}$ square matrices representing the mass, the damping, and the stiffness matrix, respectively, the last one also containing the corrective boundary terms; and $\boldsymbol{F}[\equiv \boldsymbol{F}(t)]$ is the generalized force vector represented as a $3\mathcal{J} \times 1$ column matrix.

Note that for the nonactivated beam, or when velocity feedback control is not implemented, $\boldsymbol{C}$ becomes immaterial.

Also note that the displacement and moment control only affect the stiffness matrix $\boldsymbol{K}$, whereas the acceleration and velocity control affect the mass matrix $\boldsymbol{M}$ and the damping matrix $\boldsymbol{C}$, respectively.

By multiplying Eq. (23) by $\boldsymbol{M}^{-1}$, introducing the generalized velocities $\dot{\boldsymbol{q}}$ as auxiliary variable, and defining the state-space vector $\boldsymbol{X}^T = \{\boldsymbol{q}; \dot{\boldsymbol{q}}\}$, one can express the set of governing equations (23) in state-space form:

$$\dot{\boldsymbol{X}} = \boldsymbol{A}\boldsymbol{X} + \boldsymbol{B}\boldsymbol{F} \tag{24}$$

where

$$\boldsymbol{A} = \begin{pmatrix} \boldsymbol{0} & \boldsymbol{I} \\ -\boldsymbol{M}^{-1}\boldsymbol{K} & -\boldsymbol{M}^{-1}\boldsymbol{C} \end{pmatrix}, \qquad \boldsymbol{B} = \begin{pmatrix} \boldsymbol{0} \\ \boldsymbol{M}^{-1} \end{pmatrix} \tag{25}$$

In this way, the determination of the time history of the open-/closed-loop dynamic response has been reduced to the solution of the state-space equation, that is, of a set of coupled ordinary differential equations of first order with respect to time, for which efficient numerical schemes of solution are available.

A direct evaluation of the effects of bonding imperfections on the open-/closed-loop eigenfrequency and on damping is obtained by solving the eigenvalue problem obtained from Eq. (24) by considering $\boldsymbol{F} = 0$.

Because by virtue of the control law (21) the boundary moment control is related to the kinematic response quantities, namely, $u^{(0)}$, ϕ_x, and w, and with their spatial and time derivatives, for the case of free vibrations the problem becomes homogeneous. By representing the generalized coordinates as $q_j(t) = \exp(\xi + i\Omega)t$, an eigenvalue problem that can be easily solved numerically can be obtained. Here the real and immaginary parts of the jth eigenvalue of $\boldsymbol{A}$ represent the damping and the frequency of the mode q_j, respectively.

Numerical Illustrations and Discussion

In this section, the open-loop, that is, the nonactivated, and closed-loop, that is, the activated, dynamic response characteristics of a cantilever laminated beam, as influenced by the bonding imperfections, are investigated. The free and forced flexural motions in the (x, z) plane under transient loadings $\bar{P}_z$ are studied.

The host structure is a three-layered (0-/90-/0-deg) symmetric cross-ply beam having a length-to-thicknessratio $L/h = 10$. At the top and bottom of the beam, there are thin piezoactuator layers mounted, uniformly spread over the span and subjected to an out-of-phase activation resulting in a bending moment control $\hat{M}(L, t)$. The material properties of the host structure are $E_L = 172.375$ GPa, $E_T = 6.895$ GPa, $G_{LT} = 3.448$ GPa, $G_{TT} = 1.379$ GPa, and $\nu_{LT} = 0.25$. E is Young's modulus, G the shear modulus, and ν Poisson's ratio, and subscripts L and T are the directions parallel and normal to the fibers, respectively.

As is evident, the main interest is to emphasize the implications of the interlaminar bonding imperfections on the dynamic response quantities, thus enabling one to enhance the response behavior by using a control methodology governed by the feeback law [Eq. (21)].

The top and bottom piezoactuator are polyvinilidene-difluoride (PVF)-2 layers with 40 μm thickness with the following mechanical properties: $E_L = E_T = 21.8$ GPa, $G_{LT} = G_{TT} = 8.384$ GPa, and $\nu_{LT} = 0.30$. Throughout the numerical illustrations, as a measure of bonding imperfections, the nondimensional sliding constant R is assumed:

$$R = {}^{(k)}RE_T \mid L$$

Unless otherwise stated, R is assumed to be the same at all interfaces. All computations are made for $h = 1$.

Note that the feedback gains $\mathcal{K}_{(a,m,v,w)}$ are used in normalized form $K_{(a,m,v,w)}$ as

$$K_a = \mathcal{K}_a(1 \mid E_T h^2 L), \qquad K_m = \mathcal{K}_m(1 \mid E_T h^2 L)$$

$$K_v = \mathcal{K}_v(1 \mid E_T h^2 L), \qquad K_w = \mathcal{K}_w(1 \mid E_T h^2 L)$$

and the fundamental frequency Ω normalized as ω:

$$\omega = \Omega\sqrt{\rho \mid (E_T h^2)}$$

with the layers assumed to have the same mass density ρ. The numerical results are presented in two groups. The first group is devoted to open-/closed-loop eigenfrequencies (Figs. 1–5), whereas within the second group, the time responses for free and forced motions are shown (Figs. 6–13).

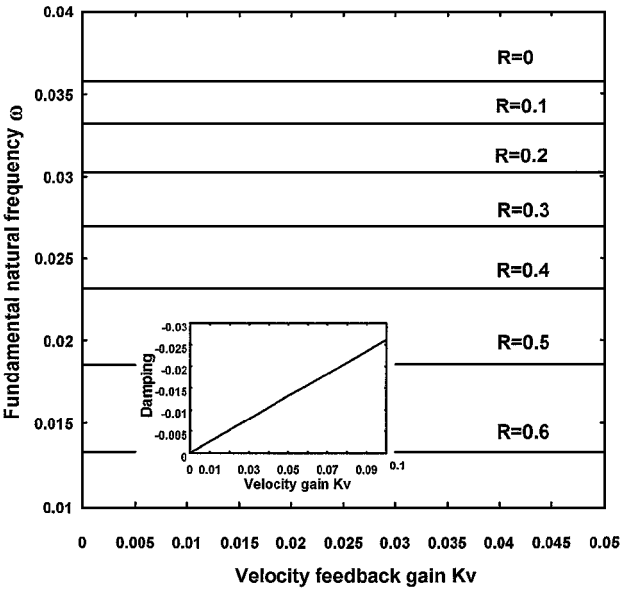

Fig. 1 Influence of the velocity feedback gain K_v on the closed-loop fundamental natural frequency of the beam featuring interlaminae bonding imperfections of selected measures R.

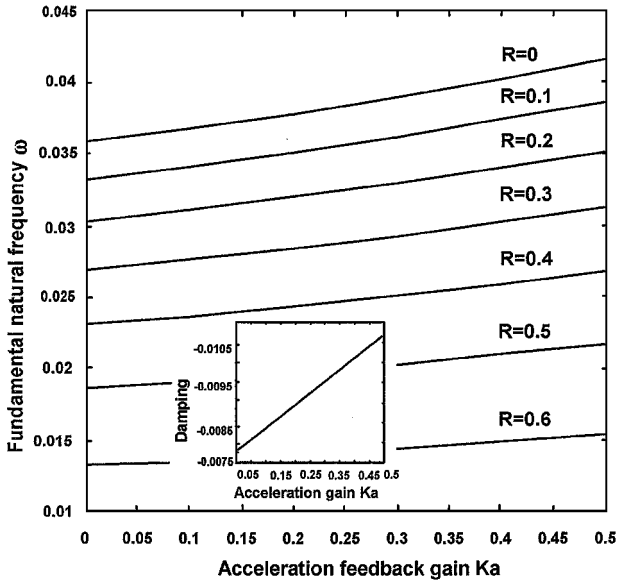

Fig. 2 Influence of the combined acceleration and velocity feedback gains ($K_v = 0.03$) on the closed-loop fundamental natural frequency of the beam featuring interlaminae bonding imperfections of selected measures R.

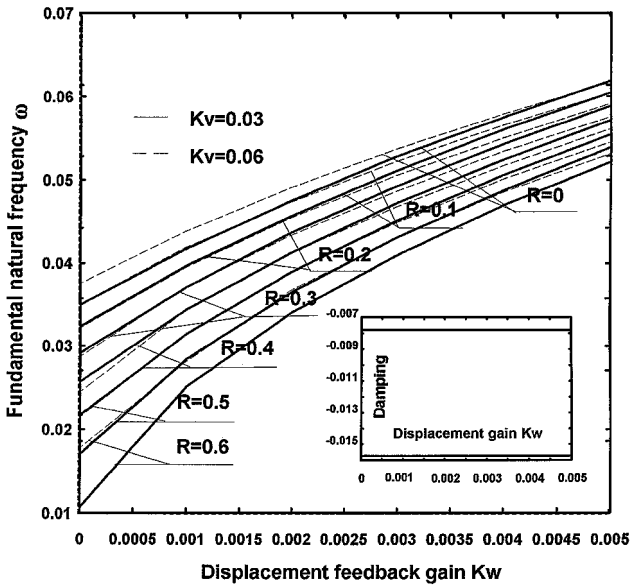

Fig. 3 Influence of the combined displacement and velocity feedback gains (K_v = 0.03 and 0.06) on the closed-loop fundamental natural frequency of the beam featuring interlaminae bonding imperfections of selected measures *R*.

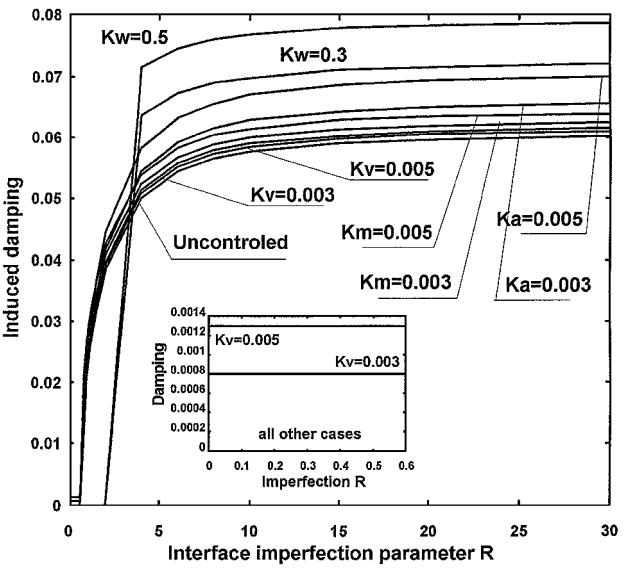

Fig. 5 Influence of the combined acceleration, displacement, bending moment, and velocity feedback gains on the induced damping of the beam featuring interlaminae bonding imperfections of selected measures *R*.

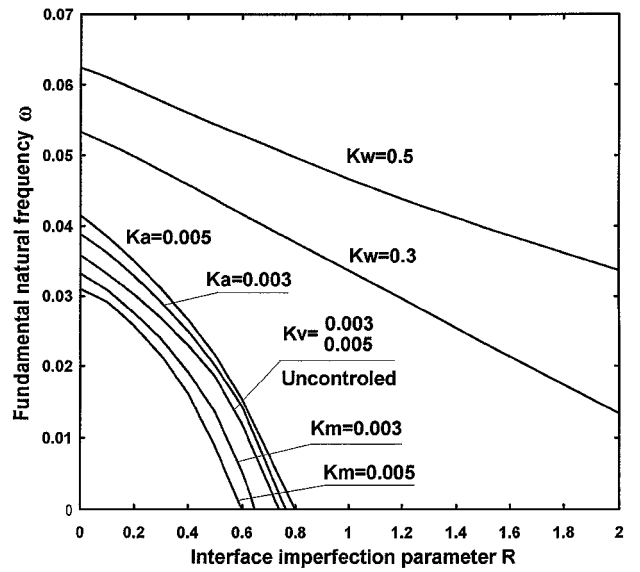

Fig. 4 Influence of the combined acceleration, displacement, bending moment, and velocity feedback gains on the closed-loop fundamental natural frequency of the beam featuring interlaminae bonding imperfections of selected measures *R*.

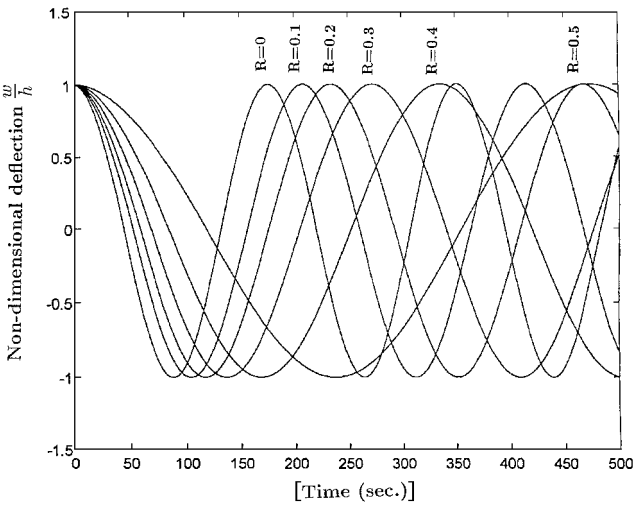

Fig. 6 Free vibration response of the unactivated beam featuring interlaminae bonding imperfections of selected measures *R*.

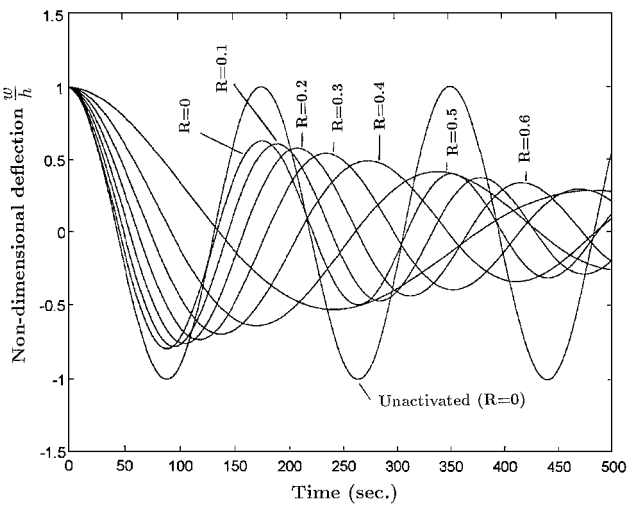

Fig. 7 Free vibration response of the activated beam (K_v = 0.01) featuring interlaminae bonding imperfections of selected measures *R*.

Figure 1 shows the open-loop, that is, unactivated, and closed-loop eigenfrequency vs the feedback gain and refers to the case of velocity control. In this case, the bending moment control at the beam tip is proportional to the tip velocity through the velocity feedback gain K_v [see Eq. (21)]. Note that, contrary to displacement, acceleration, and bending moment unifeedback control laws, in the present case the closed-loop eigenvalues are complex conjugate quantities, implying that damping is generated. The following observations are in order. It clearly appears that, as a result of bonding imperfections, a reduction of the fundamental natural frequencies is experienced for all of the investigated values of K_v. This reduction appears even for small bonding defects, that is, for the lowest values of R. At these values of R, the highest sensitivity is experienced (as revealed by the steepest gradients in the plots), and sensitivity increases in a nonproportional way with increasing R and the feedback gains.

As becomes evident from Fig. 1, the bonding imperfections, which intervene merely in the stiffness matrix $\boldsymbol{K}$, do not influence the induced damping. Thus, in such a case the dampings for the various

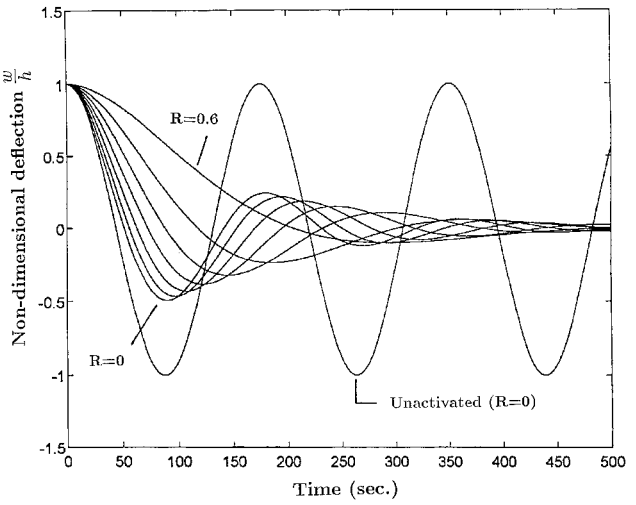

Fig. 8 Free vibration response of the activated beam ($K_v = 0.03$) featuring interlaminae bonding imperfections of selected measures R.

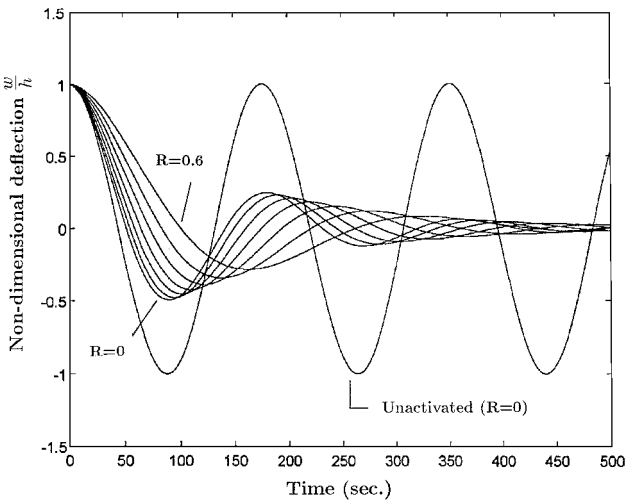

Fig. 9 Free vibration response of the activated beam ($K_v = 0.03$) featuring interlaminae bonding imperfections at one interface only.

R coincide. It is also seen that the increase of K_v, intervening merely in the matrix $\boldsymbol{C}$, affects the fundamental natural frequency.

Results, not reported for the sake of brevity, show that the same effect of reduction of the fundamental natural frequency by bonding imperfections, with the same trend as in Fig. 1, is shown for displacement, acceleration, and bending moment unifeedback control cases. As evidenced by the values of the feedback gains involved in these cases, the influence of the displacement and moment control is greater than the velocity and acceleration control over the fundamental natural frequency. Depending on the sign chosen for the feedback gains K_a, K_m, and K_w, the acceleration, bending moment, and displacement controls can contribute to an increase or the decay the closed-loop eigenfrequency. Unless otherwise stated, the sign is here chosen so as to increase the eigenfrequency.

Figures 2 and 3 show the coupled effect of acceleration and velocity (K_a, K_v) and of displacement and velocity (K_w, K_v) feedback controls, respectively. Note that within these two combined feedback control metodologies, the closed-loop eigenvalues are complex-valued quantities. Earlier conclusions are confirmed, in the sense that the eigenfrequencies decrease with the increasing of R and increase with the increase of the acceleration and displacement feedback gains. For the combined acceleration and velocity feedback control, with K_v constant, damping remains constant with the increase of K_a, until the critical value is reached and the response becomes non-oscillatory. Beyond this point the eigenvalue imaginary part, which loses its meaning of damping, still increases with increasing K_a.

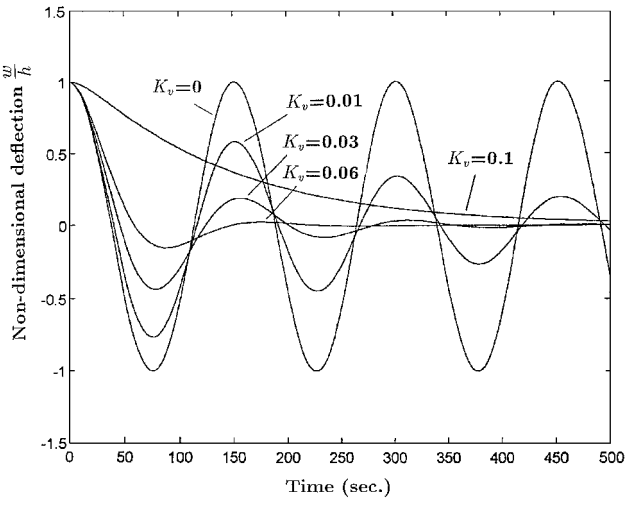

Fig. 10 Free vibration response of the activated, undamaged beam ($R = 0$) under combined control for selected measures of the velocity feedback gain ($K_v = 0, 0.1$) and $K_a = 0.5$.

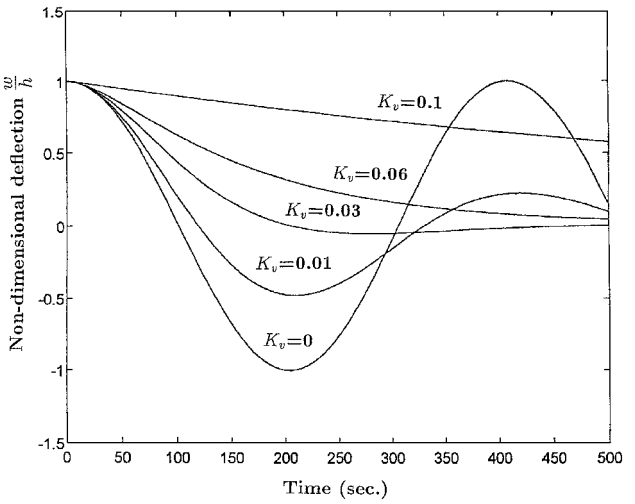

Fig. 11 Free vibration response of the activated beam with defective bonding ($R = 0.6$) under combined control for selected measures of the velocity feedback gain ($K_v = 0, 0.1$) and $K_a = 0.5$.

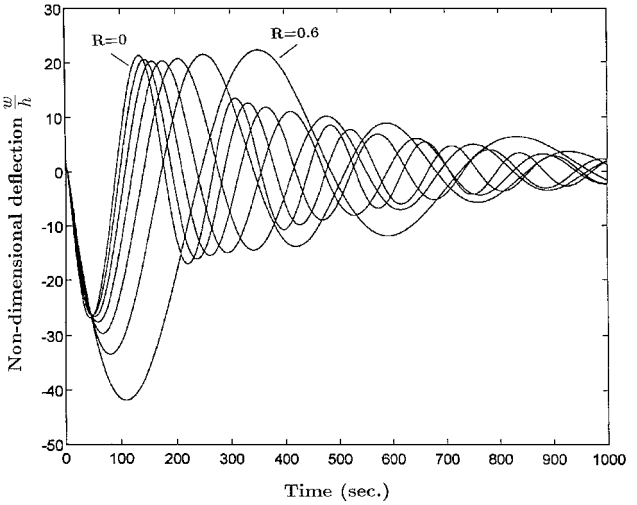

Fig. 12 Time history of the transverse deflection response under a blast pulse, of the activated beam ($K_v = 0.01$, $K_a = 0$) with defective bonding interfaces; overpressure associated with the blast pulses: $\bar{P}_z = P_m\,(1 - t/t_p)\,e^{-a'/t_p}$ ($P_m = 1.5$, $t_p = 0.1$, $a' = 0.1$).

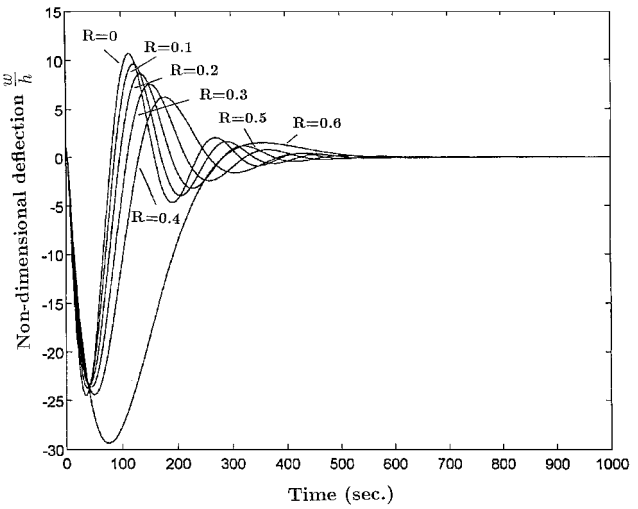

Fig. 13 Time history of the transverse deflection response under a blast pulse of the activated beam ($K_v = 0.03$, $K_a = 0.5$) with defective bonding interfaces; overpressure associated with the blast pulses: $\bar{P}_z = P_m (1 - t/t_p) e^{-a't/t_p}$ ($P_m = 1.5$, $t_p = 0.1$, $a' = 0.1$).

In the case of the combined displacement and velocity control, with K_v constant, damping does not become critical within the range of the considered values of K_w. This also gives a measure of the lower efficiency of displacement control over acceleration control. In both the earlier cases of acceleration and displacement control for fixed values of K_a and K_w, the increase of K_v results in piezoelectrically induced damping.

Figures 4 and 5 show the fundamental natural eigenfrequency, that is, the eigenvalue real part, and the damping, that is, the eigenvalue imaginary part, respectively, as a function of R, for various feedback control laws acting at once. From Fig. 4 it is seen that bonding imperfections of increasing magnitude result in reducing the fundamental frequency, irrespective of the control law, and that critical damping is reached for R ranging from 0.6 to 0.8, depending on the applied control law. It is also seen that, even in the absence of control, critical damping is reached with increasing R. The case where the sign of K_m is chosen as to decrease the fundamental natural frequency has been presented.

In Fig. 5 it is seen that, for small values of R, there is a constant damping increasing with K_v within the velocity control, the absence of damping for the other control laws acting at once, and the occurrence of critical damping for R ranging from 0.6 to 0.8, except for displacement control, which requires greater values of R. Greater efficiency of velocity, acceleration, and bending moment controls over displacement control is also seen. Beyond the jump, the eigenvalue imaginary part, which loses its meaning of damping, increases for intermediate values of R and becomes constant for the larger ones, irrespective of the control law.

Figures 6–13 concern the time response for the cases of free and forced motions. Notice that the displayed results have been generated for the case of initial conditions consisting of zero velocity and unit nondimensional deflection. To show the effects of bonding imperfections on the induced damping and frequencies, the presented results mainly concern cases where velocity control is applied.

Figure 6 shows the open-loop free vibration, as influenced by bonding imperfections. The progressive reduction of the beam stiffness resulting from the increase of bonding imperfections yields a reduction of the fundamental frequency or, in other words, results in the increase of the vibration period. Figure 6 provides the reference open-loop solution for $R = 0$ used for comparison in Figs. 7–11.

Figures 7–9 involve velocity feedback control. From these time-domain plots, results related to the increase of induced damping with increasing velocity gains and with bonding imperfections merely affecting the fundamental frequency, and thus having no effect on damping, are revealed. These findings confirm the earlier obtained results of Figs. 1, 2, and 5.

The comparison of the results of Fig. 8, where bonding defects have the same magnitude at both of the interfaces, and of Fig. 9, where only one interface is defective, shows that the effect of the damage is also dependent on its location. In fact, it is related to the distribution of σ_{xz} across the thickness [see Eq. (8)], which is influenced by the location of the damage. It is seen from Fig. 8 that where $R = 0.6$ and $K_v = 0.03$ there results critically induced damping, although the same does not occur in Fig. 9.

Figures 10 and 11 involve a combined feedback control consisting of acceleration and velocity controls. The effects of velocity control on the induced damping for an undamaged beam ($R = 0$) and for a damaged beam ($R = 0.6$) are shown. It appears that bonding imperfections, consequent to the stiffness reduction they produce, could anticipate the occurrence of nonoscillatory motions, enhancing the effects of velocity control. In the illustrated cases it is seen that for the undamaged beam the critical induced damping occurs at $K_v = 0.1$, whereas for the damaged one with $R = 0.6$, it takes place at $K_v = 0.03$.

Figures 12 and 13 show the time-history deflection response to a blast pulse. These results again reveal the powerful effect played by the velocity feedback control toward suppressing transversal deflections. Generally speaking, the same remarks in the discussion of Figs. 1–5 hold valid in the transient motion as well, where the response is dominated by the modal characteristics of the structure.

Conclusions

A number of issues related to the part played by interfacial bonding imperfections in the dynamic response of smart laminated cantilever beams have been addressed. Nonclassical effects, related to the transverse shear deformability and distortion of the normals have been included in the structural model. An efficient solution methodology for determining the open-/closed-loop dynamic response was devised. The results of this numerical investigation show that the closed-loop fundamental eigenfrequency and the time-history response are strongly affected by such imperfections. The results also reveal the powerful effect played by the nature of the feedback control in supressing the free and forced vibrations and attenuating the detrimental effect induced by interlaminar bonding defects. Although exploratory in nature, it is hoped that this study will encourage future research activity toward a better understanding of the effects played by bonding imperfections on the control of the dynamic response of laminated structures made by advanced composite materials.

Acknowledgments

Financial support of this work by the Consiglio Nazionale delle Ricerche through Grants CTB97.00589.CT11 and CTB97.00459.CT11 is gratefully acknowledged by M. Di Sciuva and U. Icardi. L. Librescu acknowledges with gratitude partial support of this research by NATO Grant CRG960118.

References

[1]Cheng, Z. Q., Jemah, A. K., and Williams, F. W., "Theory for Multilayered Anisotropic Plates with Weakened Interfaces," *Journal of Applied Mechanics*, Vol. 63, No. 4, 1996, pp. 1019–1026.

[2]Cheng, Z.-Q., Kennedy, D., and Williams, F. W., "Effect of Interfacial Imperfection on Buckling and Bending Behavior of Composite Laminates," *AIAA Journal*, Vol. 34, No. 12, 1996, pp. 2590–2595.

[3]Schmidt, R., and Librescu, L., "Geometric Nonlinear Theory of Laminated Anisotropic Composite Plates Featuring Interlayer Slips," *Nova Journal of Mathematics, Game Theory and Algebra*, Vol. 5, No. 2, 1996, pp. 131–147.

[4]Di Sciuva, M., Icardi, U., and Librescu, L., "On Modeling of Laminated Composite Structures Featuring Interlaminar Bonding Imperfections," *Advanced Methods in Materials Processing Defects*, edited by M. Predeleanu and P. Gilormini, Vol. 45, Studies in Applied Mechanics, Elsevier, New York, 1997, pp. 395–404.

[5]Di Sciuva, M., "A Geometrically Nonlinear Theory of Multilayered Plates with Interlayer Slips," *AIAA Journal*, Vol. 35, No. 11, 1997, pp. 1753–1759.

[6]Icardi, U., Librescu, L., and Di Sciuva, M., "Thermomechanical Response of Laminated Flat Panels Featuring Interlaminar Bonding Imperfections," *Analysis and Design Issues for Modern Aerospace Vehicles*, edited by G. J. Simitses, Vol. 55, ASME-AD, American Society of Mechanical Engineers, Fairfield, NJ, 1997, pp. 197–214.

[7]Crawley, E. F., "Intelligent Structures for Aerospace: A Technology Overview and Assessment," *AIAA Journal*, Vol. 32, No. 8, 1994, pp. 1689–1699.

[8]Rao, S. S., and Sunar, M., "Piezoelectricity and Its Use in Disturbance Sensing and Control of Flexible Structures: A Survey," *Applied Mechanical Reviews*, Vol. 31, No. 4, 1994, pp. 113–123.

[9]Tzou, H. S., *Piezoelectric Shells, Distributed Sensing and Control of Continua*, Kluwer Academic, Dordrecht, The Netherlands, 1993.

[10]Librescu, L., and Na, S. S., "Dynamic Response Control of Thin-Walled Beams to Blast and Sonic-Boom Using Structural Tailoring and Piezoelectrically Induced Boundary Moment," *Journal of Applied Mechanics*, Vol. 65, No. 2, 1998, pp. 497–504.

[11]Librescu, L., and Na, S. S., "Bending Vibration Control of Cantilevers Via Boundary Moment and Combined Feedback Control Laws," *Journal of Vibration and Control*, Vol. 4, No. 6, 1998, pp. 733–746.

[12]Song, O., and Librescu, L., "Bending Vibrations of Adaptive Cantilevers with External Stores," *International Journal of Mechanical Sciences*, Vol. 38, No. 5, 1996, pp. 483–498.

[13]Librescu, L., Song, O., and Rogers, C. A., "Adaptive Vibrational Behavior of Cantilevered Structures Modeled as Composite Thin-Walled Beams," *International Journal of Engineering Science*, Vol. 31, No. 5, 1993, pp. 775–792.

[14]Librescu, L., Meirovitch, L., and Song, O., "Integrated Structural Tailoring and Adaptive Materials Control for Advanced Aircraft Wings," *Journal of Aircraft*, Vol. 33, No. 1, 1996, pp. 203–213.

[15]Icardi, U., Di Sciuva, M., and Librescu, L., "Smart Structures Featuring Imperfect Bonding Interfaces: Modeling and Implications," *Proceedings of the SPIE's Fifth International Symposium, Smart Structures and Materials 1998: Mathematics and Control in Smart Structures*, SPIE Vol. 3323, edited by V. V. Varadan, 1998, pp. 202–213.

[16]Icardi, U., "Eight-Noded Zig-Zag Element for Deflection and Stress Analysis of Plates with General Lay-Up," *Composites-Part B: Engineeering*, Vol. 29b, No. 4, 1998, pp. 435–441.

[17]Di Sciuva, M., "Bending, Vibration and Buckling of Simply-Supported Thick Multilayered Orthotropic Plates. An Evaluation of a New Displacement Model," *Journal of Sound and Vibration*, Vol. 105, No. 3, 1986, pp. 425–442.

[18]Di Sciuva, M., "An Improved Shear-Deformation Theory for Moderately Thick Multilayered Anisotropic Shells and Plates," *Journal of Applied Mechanics*, Vol. 54, No. 3, 1987, pp. 589–596.

[19]Di Sciuva, M., "Multilayered Anisotropic Plate Models with Continuous Interlaminar Stresses," *Composite Structures*, Vol. 22, No. 3, 1992, pp. 149–167.

[20]Di Sciuva, M., "A Generalization of the Zig-Zag Plate Models to Account for General Lamination Configurations," *Atti Accademia delle Scienze di Torino-Classe di Scienze Fisiche, Matematiche e Naturali*, Vol. 128, No. 3–4, 1994, pp. 81–103.

[21]Icardi, U., and Di Sciuva, M., "Large-Deflection and Stress Analysis of Multilayered Plates with Induced-Strain Actuators," *Smart Materials and Structures*, Vol. 5, No. 2, 1996, pp. 140–164.

[22]Lu, X., and Liu, D., "Interlaminar Shear Slip Theory for Cross-Ply Laminates with Nonrigid Interfaces," *AIAA Journal*, Vol. 30, No. 4, 1992, pp. 1063–1073.

[23]Lavrentyev, A. I., and Rockhlin, S. I., "Ultrasonic Spectroscopy of Imperfect Contact Interfaces Between a Layer and Two Solids," *Journal of the Acoustical Society of America*, Vol. 103, No. 2, 1998, pp. 657–664.

[24]Lagnese, J. E., and Lions, J. L., "Boundary Stabilization of Thin Plates," Collection Recherches en Mathematiques Appliquees, Vol. 6, Masson, Paris, 1988.

[25]Lagnese, J. E., "Boundary Stabilization of Thin Plates," *SIAM Studies in Applied Mechanics*, No. 10, Society for Industrial and Applied Mathematics, Philadelphia, 1989, pp. 100–176.

[26]Bailey, T., and Hubbard, J. E., Jr., "Distributed Piezoelectric-Polymer Active Vibration Control of a Cantilever Beam," *Journal of Guidance, Control, and Dynamics*, Vol. 8, No. 5, 1985, pp. 605–611.

[27]Tzou, H. S., and Zhong, J. P., "Adaptive Piezoelectric Structures: Theory and Experiment," *Active Materials and Adaptive Structures*, edited by G. J. Knowles, Materials and Structures Series, Inst. of Physics Publications, Norwich, England, U.K., 1992, pp. 219–224.

[28]Baz, A., "Boundary Control of Beams Using Active Constrained Layer Damping," *Journal of Vibration and Acoustics*, Vol. 29, No. 3, 1997, pp. 166–172.

[29]Washizu, K., "Variational Methods in Elasticity and Plasticity," Pergamon, Headington, England, U.K., 1968, pp. 15–17.

A. M. Baz
Associate Editor